Near Wake of a Blunt Body at Hypersonic Speeds

C. Forbes Dewey Jr.*
California Institute of Technology, Pasadena, Calif., and University of Colorado, Boulder, Colo.

An experimental investigation was conducted to determine the characteristics of the near wake of a blunt body in hypersonic flow. Base-pressure and body-surface pressure measurements are combined with hot-wire and pitot-pressure data to describe the free shear layer, the base-flow region, the recompression zone, and the initial development of a laminar wake. It is found that the postulate of thin shear layers is valid for Reynolds numbers greater than about 10^4, if the Mach number M_e external to the shear layer is not large. Detailed measurements with a steady-state hot-wire behind a two-dimensional circular cylinder indicate that the maximum pressure rise occurs downstream of the stagnation point formed by the merging shear layers. The hot-wire measurements are corroborated by base-pressure data obtained with cylinders and wedges. Comparison between the experimental and theoretical results points out the importance of the base-flow temperature and the initial shear-layer profile in determining the observable characteristics of the near wake.

Nomenclature

H = half-height of wedge; total enthalpy, $c_pT + u^2/2$
i = hot-wire current
l = distance measured along shear layer
L = characteristic body length
M = Mach number
p = static pressure in flow; model surface pressure
p_b = base pressure at model centerline
p_{t2} = total (stagnation) pressure behind normal or oblique shock; pitot pressure behind normal shock
R = wire resistance
Re = Reynolds number $\rho ux/\mu$, where x is characteristic distance
s = distance along dividing streamline from separation
T = temperature
u = local flow velocity
x = distance in streamwise direction from centers of cylinders and spheres or bases of cones and wedges
y = distance from model axis in transverse direction
α_r = temperature-resistivity coefficient, $(R_w/R_r) = 1 + \alpha_r(T_w - T_r)$
δ = boundary-layer or shear-layer velocity thickness; δ^* = displacement thickness
θ_w = wedge half-angle
θ_0 = initial momentum thickness of the shear layer
μ = viscosity
ξ = shear-layer variable $(s/\theta_0)^2(1/Re_{e,s})$
ρ = density
ψ = stream function

Subscripts and Superscripts

$(\ )_b$ = evaluated in base-flow region
$(\ )_e$ = quantity at outer edge of boundary layer or shear layer
$(\ )_0$ = evaluated at stagnation temperature
$(\ )_*$ = quantity along dividing streamline
$(\ )_\infty$ = freestream quantity
$(\ )_B$ = quantity evaluated along body surface in upstream attached flow region
$(\ )'$ = conditions at edge of wake downstream of neck

Presented as Preprint 64-43 at the AIAA Aerospace Sciences Meeting, New York, N. Y., January 20–22, 1964; revision received November 17, 1964. This work was carried out under the sponsorship and with the financial support of the U. S. Army Research Office and the Advanced Research Projects Agency, Contract No. DA-31-124-ARO(D)-33. This research is a part of Project Defender sponsored by the Advanced Research Projects Agency. I am indebted to Lester Lees for his guidance and inspiration and for the support that he and Clark Millikan gave to the present investigation. I also wish to thank Toshi Kubota, who was always ready to offer his constructive advice.

* National Science Foundation Fellow, California Institute of Techno ogy, Pasadena, Calif.; presently Assistant Professor, Aerospacel Engineering Sciences, University of Colorado, Boulder, Colo. Member AIAA.

Introduction

THE wake of a blunt body at low speeds is complicated by the existence of a time-dependent flow field. Roshko[1, 2] found that vortices are developed behind the body, the dominant frequency being proportional to the freestream velocity. This periodicity is also present in the investigations of Gorecki,[3] Nash,[4] Thomann,[5] and Gowen and Perkins[6] at subsonic speeds. In the experiments cited previously, the test body was two-dimensional, but similar results have been found for spheres in subsonic flow.[7–9]

As the freestream Mach number M_∞ is increased, a drastic change occurs in the structure of the base region. For $M \gtrsim 1$ (the exact value varies with geometry and Reynolds number), the violent periodic behavior evidenced at lower speeds disappears, and a steady supersonic flow pattern is established. Figure 1, reproduced from the work of Nash,[4] clearly indicates the dramatic change which occurs in the wake structure. Similar phenomena are evident in the schlieren photographs of spheres by Charters and Thomas,[9] of cones by Charters[10] and by Pallone, Erdos, and Eckerman,[11] and of cylinders by Thomann.[5]

Further increases in Mach number at large body Reynolds numbers produce no qualitative change in the near wake.† This is explained by the well-known "hypersonic freeze" or "Mach number independence principle,"[12] which recognizes that the viscous and inviscid flow fields become independent of Mach number if $M_\infty \sin\theta_B$ is sufficiently large (θ_B is the characteristic angle between the freestream direction and the local body surface). Thus, the flow field about a blunt body will be "frozen" at a much lower value of freestream Mach number than that which pertains to a slender body.

Decreasing the Reynolds number at a fixed value of M_∞ will produce a laminar boundary layer on the surface; as the boundary layer separates to become the shear layer, it will remain laminar if the Mach number M_e at its outer edge is greater than about 2.5.[13] The two shear layers from opposite sides of the body then meet to form a laminar viscous wake, which may persist for many body diameters in the

† For many body diameters downstream, the inviscid wake exhibits a static enthalpy profile which depends strongly on Mach number if $M_\infty \gg 1$.

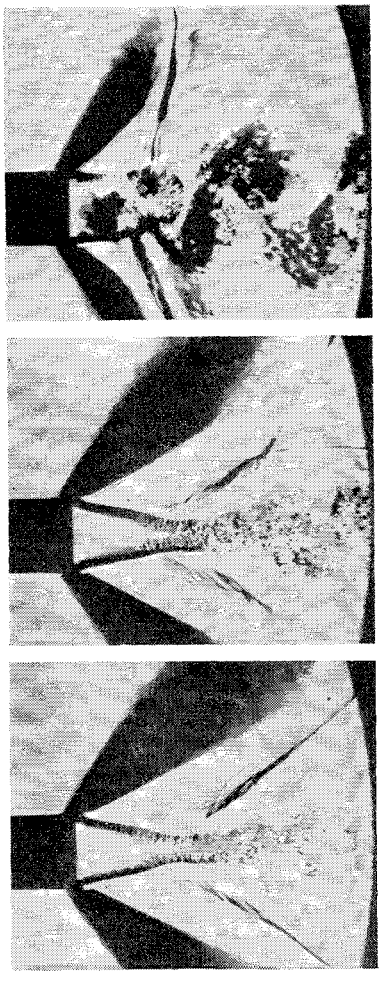

a) M = 0.925

b) M = 1.00

c) M = 1.05

Fig. 1 Base flow behind a slender two-dimensional body at transonic speeds.

downstream direction.[11, 13–18] Thus, there exists an important class of wake flows for which the shear processes are laminar and time-independent.

Section I describes a detailed model of the steady laminar near wake that follows from the requirement of mass conservation in the recirculation region and the assumption of momentum conservation along the dividing streamline in the immediate vicinity of the wake neck. The shear-layer velocity profile is found to differ significantly from the similarity profile for constant-pressure mixing. In Section II, the importance of the initial shear-layer profile is described. The experimental methods used in this investigation are recorded in Section III, whereas measurements of surface and base pressures are presented in Section IV, and mass-flow and total temperature profiles across the wake are given in Section V. Finally, a rapid technique for mapping out the qualitative features of the near wake is proposed in the Appendix.

I. Physical Model of the Flow Field

Historically, the two most important contributions to a model of the near wake were 1) the observation that mass conservation requires all of the fluid originally within the base-flow region and entrained by the shear layer to be returned to the base region at the wake neck, and 2) a recognition of the dominant role of the shear-layer mixing rate in determining the pressure rise required to satisfy the mass conservation condition. The mass conservation condition was first proposed by Chapman,[19] and the role of the shear-layer mixing process was originally expounded by Crocco and Lees.[20] (Several difficulties appearing in the Crocco-Lees model have been recently clarified by Glick.[21]) The first successful quantitative prediction of base-flow phenomena was given by Chapman for laminar flow (see Refs. 22–24) and Korst, Page, and Childs[25] for the case of a turbulent shear layer.

Figure 2 defines the physical model, which follows from the assumptions of mass conservation and momentum conservation along the dividing streamline. Under the influence of viscous and pressure forces, the boundary layer separates from the body to form a viscous mixing layer of length l. This layer entrains mass from the external inviscid region (subscript e) and also along the lower boundary bordering the base-flow region. As the shear layer grows, the velocity u_* and Mach number M_* along the "dividing streamline" ($\psi = 0$) increase because of momentum transfer.

In order to conserve mass, all of the streamlines below $\psi = 0$ must be turned back into the base region by the compression at the neck, and all of the particles following streamlines $\psi > 0$ will pass through the neck and flow downstream, although at a reduced velocity. Conservation of mass and momentum, therefore, specify the pressure rise $(p' - p_e)$ required to bring the dividing streamline to rest.

If the Reynolds number $Re_{e,l} = (\rho_e u_e l/\mu_e)$ is large, then the shear layer is very thin. The readjustment regions in the vicinity of the separation point and the wake neck are only a few shear-layer thicknesses in extent‡ and are small if $Re_{e,l}$ is very large. In this case, constant-pressure mixing should represent a good approximation to the actual shear-layer mixing process since the amount of flow entrained by the shear layer and the dynamic pressure and velocity in the base region are small. Chapman[22] obtained a limiting solution to the constant-pressure mixing problem for $\theta_0 \to 0$. The momentum equation reduces to that of Blasius, with the boundary conditions $u \to u_e$ as $y \to \infty$ and $u \to 0$ as $y \to -\infty$, and processes a similarity solution of the form $(u/u_e) = f[y(\rho_e u_e/\mu_e s)^{1/2};\ M_e]$. In particular, he found the zero-streamline velocity ratio (u_*/u_e) to be a constant. If the initial shear-layer momentum thickness θ_0 is not small, then the velocity profile will differ significantly from Chapman's similar solution; the velocity u_*, the Mach number M_*, and the pressure rise $(p' - p_e)$ will be less than the values obtained from the similarity analysis.

Specification of the initial shear-layer momentum thickness θ_0, when combined with a knowledge of the shear-layer mixing rate and a description of the recompression process at the neck, is sufficient to define the complete flow field in the near wake. If the shear layer is thin, the mixing process may be approximated by the laminar mixing of a uniform stream and a fluid at rest. A Karman momentum integral solution to this problem is given in Ref. 27, and an equivalent numerical solution was obtained by Denison and Baum.[2] For given values of M_e, the total enthalpy ratio (H_e/H_b) and γ, the results show that the velocity ratio (u_*/u_e) and Mach number ratio (M_*/M_e) depend upon the single parameter

$$\xi \equiv (s^2/\theta_0)(1/Re_{e,s})$$

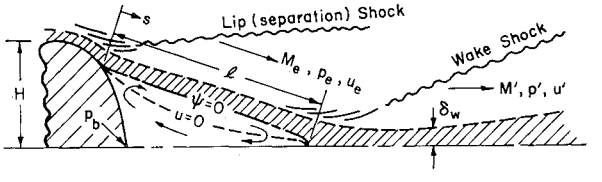

Fig. 2 Nomenclature for the near wake.

‡ This result is not obvious a priori but may be inferred from the measurements presented here. A recent study by Herzog has shown that mass injection into the base region significantly increases the extent of the recompression region and decreases the strength of the wake shock.

where $Re_{e,s} = (\rho_e u_e s/\mu_e)$ is the Reynolds number based on conditions along the outer edge of the shear layer and the distance s along the dividing streamline from the point of separation. H_b is the total enthalpy of the base region.

Crocco and Lees[20] have shown that the laminar recompression process is a function of Reynolds number, but this dependence has been found empirically to be weak in many cases. A limiting case would be that proposed by Chapman[24]: an inviscid compression of the dividing streamline. In the absence of viscous effects during separation, $(\theta_0/D) \sim (Re_{\infty,D})^{-1/2}$ and the value of $\xi(s)$ are independent of the freestream Reynolds number for any specific shear-layer geometry. The orientation of the shear layer also determines the external Mach number M_e and the turning angle of the inviscid flow at the wake neck. If Chapman's assumption[24] of inviscid recompression is adopted, and if it is further assumed that the base-flow enthalpy H_b is independent of the freestream Reynolds number, then the base pressure and structure of the near wake are also independent of Reynolds number.[29]

In summary, the original result of Chapman,[24] which predicted that the base pressure and wake angle are independent of Reynolds number, is now extended to the case of finite initial shear-layer thickness. With certain reservations, this result is applicable to axisymmetric bodies as well.[29]

The most questionable assumption embodied in this result is that of inviscid recompression. A recent study of a class of similar problems by Lees and Reeves[30] has shown that the magnitude of the allowable pressure rise at the neck (and hence the base pressure) varies with Reynolds number. The base-pressure variation for a two-dimensional cylinder predicted by the methods of Lees and Reeves[30] is in good agreement with the data to be reported in this paper. The assumption of inviscid recompression is greatly in error if the extent of the recompression region is comparable to the length of the shear layer (e.g., very low Reynolds numbers, large external Mach numbers M_e, and fluid injection into the base region[26]).

Reynolds number independence leads to a simple scaling law for the initial wake "thickness" δ_w (Fig. 2). Since $\xi(l)$ is constant, the ratio $\delta(l)/\delta_0$ is also constant, and an inviscid recompression demands that $\delta_w/\delta(l)$ be a function only of p'/p_e and M_e. At a fixed value of M_∞, therefore,

$$\delta_w \sim \delta_0 \sim (Re_{\infty,\,D})^{-1/2}$$

Figure 3 verifies this conclusion for a circular cylinder in hypersonic flow. The pitot-pressure measurements of McCarthy[31] and the diffusion profiles of Kingsland[32] confirm these schlieren results, although the wake "thickness" must be defined in a somewhat different manner for each method of observation.

The fact that the base pressure $p_b(M_\infty)$ is independent of Reynolds number means that, for blunt bodies at hypersonic speeds, (p_b/p_{t_2}) is independent of both the freestream Mach

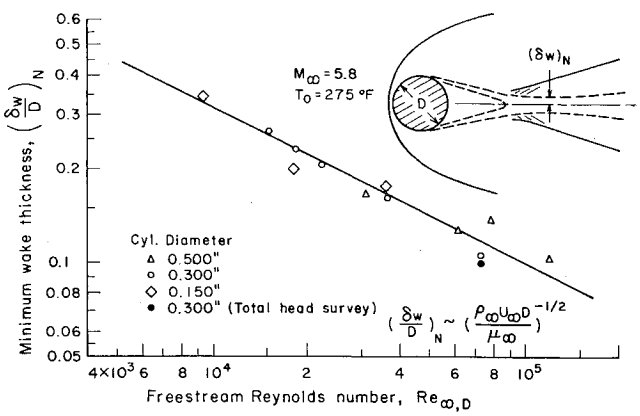

Fig. 3 Initial wake thickness from schlieren observation.

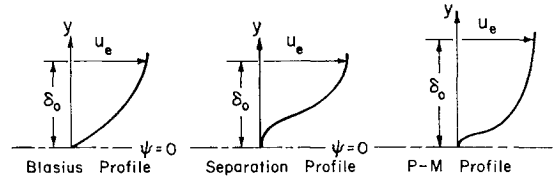

Fig. 4 Three possible shear-layer initial profiles.

number and Reynolds number. (The quantity p_{t_2} is the stagnation pressure behind the leading-edge shock wave.) The cylinder surface-pressure distributions measured by McCarthy,[31] Tewfik and Geidt,[33] Walter and Lange,[34] and Gregorek and Kordan[35] show that the pressure distribution (p_B/p_{t_2}) from the forward stagnation point to separation is identical for all of the values of $M_\infty \gtrsim 4.5$. Measurements of cylinder base pressures will be given presently which confirm that (p_b/p_{t_2}) is also approximately independent of M_∞ for $M_\infty \gtrsim 4.5$.

II. Free Shear Layer

The momentum integral method presented in Ref. 27 is only one of several alternative approaches to the constant-pressure mixing problem. The Crocco-Lees[20] mixing theory and the numerical finite-difference scheme of Denison and Baum[28] are other examples. A fundamental similarity between all of the methods is that, once an initial profile at $s = 0$ and the boundary conditions (including H_b) have been specified, the solution depends only upon the independent variable ξ.

Several general conclusions may be drawn from the numerical results reported in Ref. 27. First, the value of u_* will be considerably less than that given by $\xi \to \infty$ in most physical situations. Second, the value of $u_*(\xi)$ is sensitive to the initial profile of the shear layer. And finally, the value of u_* (and consequently the base pressure, external Mach number M_e, and shear-layer thickness) depends strongly upon the details of the separation process if $\xi = 0(1)$.

Consider three possible initial profiles with the same values of u_e and θ_0 (Fig. 4). The "Blasius" profile may be regarded as a hypothetical separation in which no interaction between the inviscid flow and viscous flow has occurred. The "separation" profile is associated with a gradual separation in an adverse pressure gradient. The Prandtl-Meyer (P-M) profile is typical of the fat velocity distribution, which would result from a sharp corner separation that includes a Prandtl-Meyer expansion fan.[36] Figure 5 shows that the Blasius profile will have a large value of u_* for small ξ because of the finite shear at the axis; initially, $u_* \sim s^{1/2}$ for a separation profile, whereas $u_* \sim s^{1/3}$ for a Blasius profile. Soon the P-M value of u_* begins to grow explosively because of the high rates of shear in the lower portions of the profile. Finally, the spreading of the high vorticity in the outer portions of the separation profile will begin to be felt at the axis, and

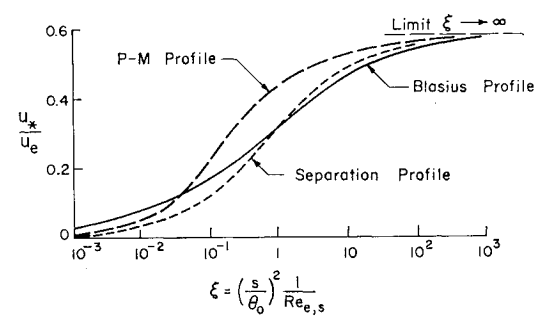

Fig. 5 Effect of initial profile on the zero streamline velocity (schematic).

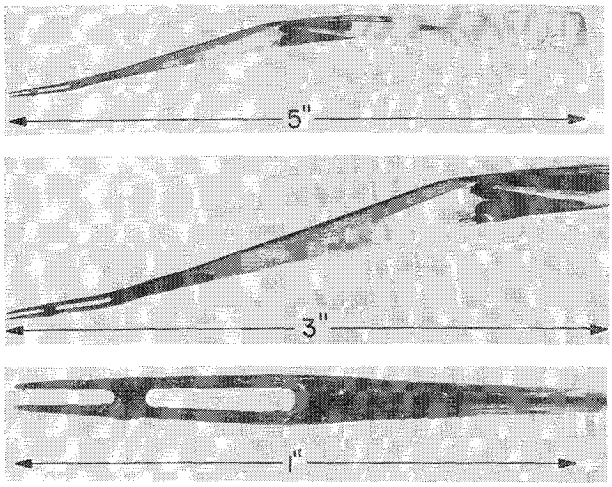

Fig. 6 Three views of the hot-wire probe.

u_* will also grow rapidly for this case. The growth rates shown in Fig. 5 explain the failure of solutions based on a Blasius-type profile to predict a value of u_* as large as the one that is experimentally observed. Lees and Reeves[30] found an analogous result in investigating the interaction between an attached boundary layer and an incident shock wave.

Strong cooling of the base region increases (M_*/M_e) and consequently increases the pressure rise (p'/p_e), which may be substained at the neck. The stagnation temperature along the zero streamline, and hence the static temperature on the axis just downstream of the wake neck, is independent of ξ only in one case: adiabatic flow. In the limiting case considered by Chapman,[22] $\xi \to \infty$ so that H_* must be equal to or greater than $(u_*/u_e) \cdot H_e$, which is 0.587 H_e for $\xi \to \infty$. This fact was pointed out by Lees and Hromas.[37] If, however, $H_b \ll H_e$ and $\xi = 0(1)$, then both u_* and the total enthalpy H_* at the neck will be considerably less than their asymptotic values.

For a highly cooled re-entry vehicle with $M_\infty \gg 1$, the body temperature is a small fraction of the freestream stagnation temperature. If the base region is to remain cool, the energy entrained between separation and recompression by that portion of the shear layer below $\psi = 0$ must be continually removed by heat transfer to the base of the body. This implies that the heat-transfer rate at the base, and hence H_b, will vary with Reynolds number so that a variation of wake characteristics (in particular the initial enthalpy defect of the wake) with Reynolds number should be expected for a highly cooled body.

III. Experimental Considerations

The experiments were carried out in leg 1 of the Graduate Aeronautical Laboratories, California Institute of Technology (GALCIT) hypersonic wind tunnel. The test section is 5 in. square, and contoured nozzle blocks produce a test section Mach number of 6. The test rhombus of uniform flow is 3 in. wide and 15 in. long, with a static-pressure uniformity better than $\pm 1.6\%$ over any cross section. Because of sidewall boundary-layer growth, the Mach number varied from 5.88 to 6.09 with freestream Reynolds number, and appropriate corrections were made to account for this effect. All of the data were obtained at stagnation temperatures sufficient to avoid air liquefaction. Automatic regulators maintained a constant stagnation temperature within $\pm 2°$F and a constant supply pressure within ± 0.07 psi. Temperatures of all of the instruments were monitored continuously, and suitable calibrations were employed to eliminate errors caused by temperature drift.

Pressure Instruments

Absolute pressure measurements were made with a U-tube micromanometer filled with Dow Corning DC 200 silicone oil and a Statham Model PA208-TC (0–5 psia) pressure transducer. The micromanometer was referenced to a pressure of 0.5 μ Hg, and had an over-all accuracy and a repeatability of about $\pm 3\mu$ Hg. For the pressure transducer operating in the range of 0–60 mm Hg, the combined hysteresis and nonlinearity was less than ± 0.06 mm Hg.

Pitot probes were manufactured from 0.028-in.-diam stainless-steel tubing and Pyrex. The stainless probe was flattened to an over-all height of 0.0116 in., an over-all width of 0.0408 in., and a wall thickness of about 0.001 in. The leading edge was squared off normal to the probe axis. Round glass pitot probes were drawn from 6 mm o.d. $\times$ 4 mm i.d. Pyrex tubing. By heating the glass to the softening point and deftly pulling it like a piece of taffy, tubes as small as 0.003 in. in o.d. could be fabricated. All of the glass probes had a gradual taper of about 5° from the tip to a uniform section of 0.020–0.025 in. in o.d.

Hot-Wire Instruments

The hot-wire probes were designed to have a minimum cross-sectional area normal to the flow direction. They consisted of a small cone-cylinder-flare body, a thin streamlined strut, and two sewing needles to hold the wire. Three views of the probe are shown in Fig. 6. The strut holding the needles was a "sandwich" of two 0.020-in.-thick blades of hard brass shim stock joined with a thin layer of Stycast 2850GT cement. This bonding agent was chosen for its low thermal expansion coefficient (about 15×10^{-6}/°C) and high electrical resistivity (10^{13} ohm-cm at tunnel operating temperatures). The needles were soft-soldered to the brass blades, and a minute bridge of Stycast 2850GT was placed halfway down the needles to increase their rigidity.

The hot wires were soft-soldered to the needles within 0.001 in. of the tips, and care was exercised to insure that the hot wires were normal to the flow direction. Pt-10% Rh Wollaston wire of 0.0001 in. diam was used as the hot-

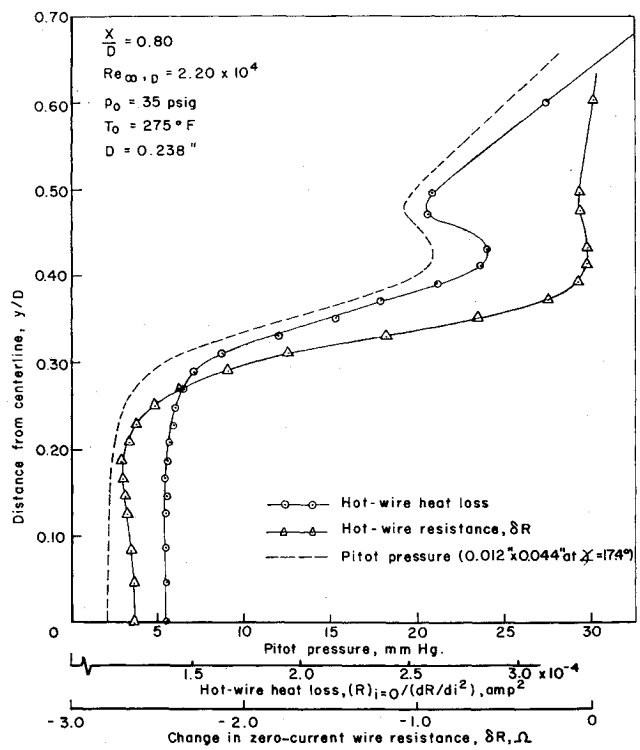

Fig. 7 Comparison between measured hot-wire and pitot-pressure profiles.

wire material, and each wire was annealed and accurately calibrated. All of the wires were obtained from a single spool, and the mean resistivity coefficient was 1.657×10^{-3} °C^{-1} at 0°C. Absolute wire resistances were measured to ± 0.01 Ω using a standard Wheatstone bridge circuit. The current through the hot wire was determined by measuring the voltage drop across a fixed resistor in series with the hot wire and was accurate to $\pm 0.05\%$.

Wind-Tunnel Models

All of the models were inserted into the tunnel through Lucite plugs mounted in a glass port. Four circular cylinders and four wedges were used in this investigation; their characteristics are detailed in Ref. 29.

Flow-Interference Effects

Serious attention was given to the effect of probe interference on the base-flow field. The most sensitive measure of these interference effects was found to be the base pressure. The hot-wire probe affected the base pressure by less than 1% outside the region $-0.7 < y/D < -0.2$. (A value $y < 0$ means that the probe was inserted completely across the wake.) For this reason, only hot-wire data for $y > 0$ were used. The pitot probe presented little disturbance to the flow field, and the pressure data were therefore read from the pitot trace for values of $y < 0$, since the probe was aligned with the flow in this region. It was not necessary to correct the hot-wire or pressure data for these interference effects. A detailed discussion of other possible sources of error is given in Ref. 29.

Experimental Techniques

Base pressures and cylinder surface pressures were measured with the silicone U-tube micromanometer. The cylinder angle of rotation was determined by a mechanical counter having 5000 divisions for 360° rotation. The centerline for the cylinder base-pressure and surface-pressure studies was determined by symmetry; this procedure was highly satisfactory.

Hot-wire and pitot-pressure surveys behind the 0.238-in.-diam cylinder were accomplished by mounting the probes on a traversing system capable of motion in the vertical and horizontal directions. Thus, "slices" could be taken at any streamwise station along the tunnel centerline. The vertical wake centerline was determined by symmetry, and this procedure yielded a repeatability of about ± 0.001 in.

The axial position behind the cylinder was determined with the aid of the two "goal-post" needles attached to the model. The tips of these needles, which extended 0.0501 ± 0.0002 in. above the model surface and were 0.5 in. apart, were rotated to the rear of the body and used as a "gunsight" to align the probe. By using a magnifier, the axial position could be consistently reset to ± 0.0015 in. while the tunnel was operating.

The pitot-pressure and hot wire data gave a consistent and complementary description of the flow field. Figure 7 reports the measured pitot pressure, hot-wire heat loss, and zero-current wire resistance measured at $x/D = 0.80$. Equivalent sets of data were obtained at several downstream stations and at four different Reynolds numbers with similar results.

Data Reduction Procedures

The data reduction procedures used in this investigation were similar to those employed previously.[38] For small wire-heating currents, R_w is a linear function of the Joulian heating i^2R_w. By plotting R_w as a function of i^2R_w, the slope $[dR/d(i^2R)]_{i=0}$ and the zero-current intercept $R_{i=0}$ could be found. The absolute values of $R_{i=0}$ and $[dR/d(i^2R)]_{i=0}$ are believed to be accurate to $\pm$ 0.02 Ω (i.e., $\pm 0.06\%$) and $\pm 4\%$, respectively.

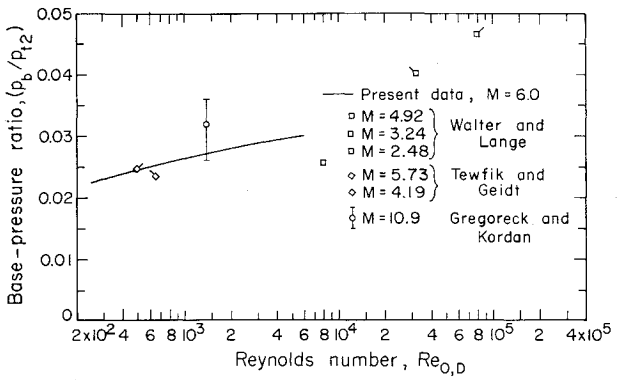

Fig. 8 Correlation of cylinder base pressures in supersonic and hypersonic flow.

IV. Base-Pressure Measurements at Hypersonic Speeds

Cylinder Base Pressures

The base pressure of a two-dimensional circular cylinder at a freestream Mach number of 6 is shown in Fig. 7. It may be seen that the aspect ratio§ required to render the ratio (p_b/p_{t_2}) independent of cylinder diameter is on the order of 20, although the errors are not large for $\mathcal{AR} \sim 10$.

According to the Mach number independence principle, the ratio (p_b/p_{t_2}) should be independent of M_∞ if $M_\infty \gg 1$. In Fig. 8, the present experiments are compared with the results of Tewfik and Geidt,[33] Walter and Lange,[34] and Gregorek and Kordan.[35] It is apparent that the flow field at the rear of the cylinder is independent of Mach number for $M_\infty \gtrsim 4$. (The scatter of other data about the present measurements is attributed in part to aspect ratio effects.)

The simplified model of the near wake predicts that the base-pressure ratio (p_b/p_{t_2}) is also independent of the Reynolds number $Re_{0,D}$. Although this is not exactly true, as indicated by Fig. 9, it is certainly a good first approximation inasmuch as the base pressure changes by 30% over a 20-fold range of Reynolds numbers. An increase in base pressure with Reynolds number was also found by Kavanau,[39] who studied an axisymmetric cone-cylinder model. The small variations of base pressure with Reynolds number seem somewhat surprising in view of the low Reynolds numbers $Re_{0,D}$. For values $Re_{0,D} \lesssim 10^4$, the shear-layer thickness is a significant fraction of the body diameter, and many of the assumptions of the base-flow model become questionable.

To compare the measured base pressures with the quantitative results of Ref. 27, it is necessary to estimate the momentum thickness θ_B on the body ahead of the separation point and determine the change in θ across the separation region. An estimate of θ_B may be obtained by the method of local similarity, using the relations derived in Ref. 40, the cylinder surface temperature found in Ref. 41, and the surface-pressure measurements given in Ref. 31.

It is found[29] that the parameter $\xi(l)$ is proportional to I_2^{-2}, where I_2 is the momentum thickness integral across the boundary layer. I_2 depends on the local pressure gradient β, which varies monotonically from unity at the stagnation point to nearly 13 at 120°. From an extrapolation of the results of Beckwith and Cohen,[42] the value of I_2 for $\beta = 13$ is 0.11. This is a factor of 4 less than the classical Blasius value for $\beta = 0$, a difference of a factor of 16 in ξ. If the body is highly cooled, then I_2 is a weak function of the pressure-gradient parameter and remains close to the Blasius value of 0.4696[43].

§ The aspect ratio is defined as the ratio of spanwise uniform flow length to cylinder diameter.

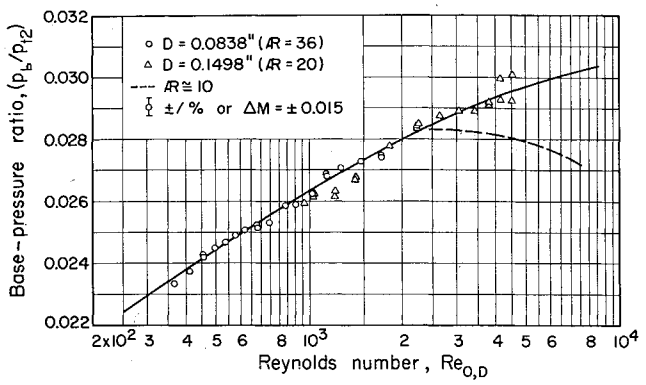

Fig. 9 Variation of cylinder base pressure with Reynolds number.

Table 1 presents the values of M_e, base pressure, and shear-layer turning angle calculated for exponential, quadratic, and Blasius initial shear-layer profiles, assuming the initial momentum thickness θ_0 to be identical to the momentum thickness on the body before separation and using an isentropic inviscid flow from the 90° point on the body through the recompression region. A comparison between the tabulated values and the experimental data of Figs. 7 and 9 indicates that the results obtained using local similarity ($\beta = 13$) are in closer agreement with experiment than the values calculated by ignoring the pressure-gradient term. The results obtained by using Chapman's solution for $\xi \to \infty$ are in better agreement with experiment than more realistic calculations that take the initial shear-layer thickness into account.

The failure of the theory may be attributed to three primary effects: 1) the lack of an accurate description of the initial momentum thickness θ_0; 2) the shear layer at low Reynolds numbers is no longer thin, and the assumptions of constant-pressure mixing and negligible base flow are violated; and 3) the pressure rise $(p' - p_e)$ depends upon viscous effects in the neck region during recompression.[30, 44]

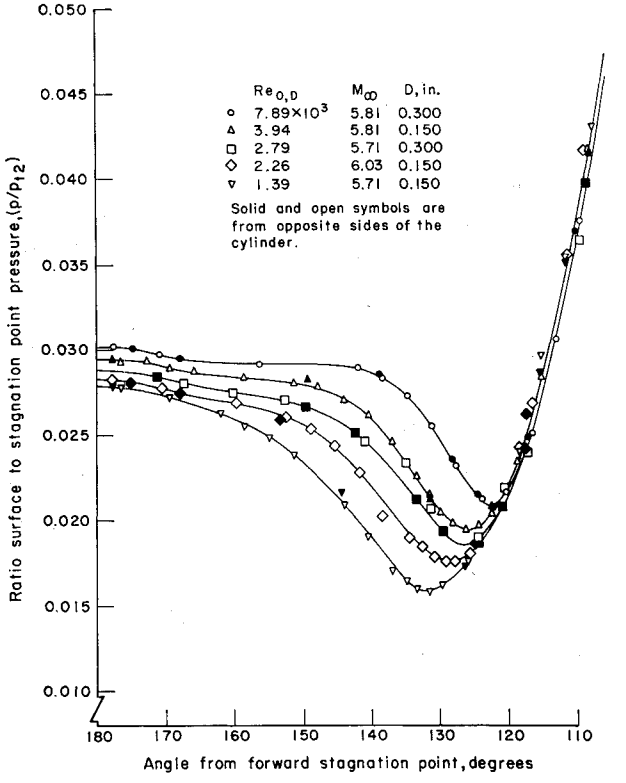

Fig. 10 Surface pressure in the region of separation.

Cylinder Surface Pressures Near Separation

Figure 10 presents the measured surface-pressure distribution on a circular cylinder as a function of the Reynolds number $Re_{0,D}$. The most striking feature is the diminishing extent and, finally, the disappearance of the region of constant surface pressure with decreasing Reynolds number. The assumption of constant-pressure mixing implies that the surface pressure aft of the separation region is constant and equal to the value at the outer edge of the shear layer. Clearly, this assumption is invalid at the lowest Reynolds numbers shown in Fig. 10, but a large region of constant pressure would be anticipated for $Re_{0,D} \gtrsim 5 \times 10^4$.

A second important result is that the separation point moves aft with decreasing Reynolds number. Both theoretical and experimental evidence indicates that the separation point is located very close to the surface-pressure minimum. The pressure rise required to separate the boundary layer increases with decreasing Reynolds number, allowing the boundary layer to penetrate more and more deeply into the base region.

The third significant item in Fig. 10 is the small pressure rise at the rear of the cylinder. This region of increased pressure extends about ±15° on either side of the axis, suggesting a stagnation of the reverse flow in the base region. If the pressure plateau for $Re_{0,D} = 7.89 \times 10^3$ is taken to be the true static pressure, and the pressure rise at the rear stagnation point is identified with the dynamic head of the reverse flow, then the Mach number of the reverse flow along the axis is 0.3.

Wedge Base Pressures

As shown in Figs. 11 and 12, the base pressure of a wedge is a strong function of Reynolds number. The measured base pressures are normalized with respect to the stagnation pressure behind the leading-edge shock wave, and the Reynolds number $Re_{2,L}$ is based on the velocity, density, and viscosity of the inviscid flow along the wedge surface and the wedge surface length L. A small (less than 10%) correction was made to account for hypersonic viscous interaction effects.[12, 40]

Three higher-order systematic effects were possible in the wedge base-pressure data. First, the freestream Mach number varied from 5.88 to 6.09 with tunnel pressure level. Solid points indicate a freestream Mach number of 6.04; three such points were available for each model. The "tailing off" of the data with decreasing Reynolds number is attributed to the small change in freestream Mach number. Second, the Mach number M_e is estimated to be between 8 and 9, so that the static temperature T_e was below the condensation limit. Tests at three stagnation temperatures showed no detectable condensation effects. Finally, the base pressures were well below the freestream pressure, and aspect ratio effects were possible. Small triangular fences were attached perpendicular to the base of the 0.30-in. base height, 22.5° wedge just outside the tunnel-wall boundary layers. As shown in Fig. 12, the difference between the

Table 1 Theoretical predictions for an insulated cylinder

Shear-layer profile	Base pressure, (p_b/p_{t2})		Turning angle, deg		M_e	
	$\beta = 13$	$\beta = 0$	$\beta = 13$	$\beta = 0$	$\beta = 13$	$\beta = 0$
Exponential[27]	0.039	0.053	10.7	6.3	2.77	2.56
Quadratic[27]	0.043	0.058	9.4	5.1	2.71	2.51
Blasius (Numerical)[29]	0.046	0.063	8.5	3.7	2.66	2.45
Chapman[24] ($\theta_0 = 0$)	0.035		12.3		2.84	

base pressures with and without fences was only 3%. More importantly, the qualitative features of the base-pressure/Reynolds number relation were not changed by these inserts.

The strong dependence of wedge base pressure on Reynolds number can be easily explained. The shear-layer Mach number M_e is between 8 and 10, so that the base pressure is a sensitive function of the shear-layer angle. The incompressible and compressible mixing problems are related through the Howarth transformation (y is in the compressible plane, and $\bar{y}$ is the transformed variable). Thus

$$y = \int_0^{\bar{y}} \left(\frac{\rho_e}{\rho}\right)$$

In the hypersonic shear layer, $(\rho_e/\rho) \gg 1$ and the lower portion of the shear layer penetrates far into the interior of the base region. It is apparent that two hypersonic shear layers will interact strongly in the neck region, and the assumption that the shear-layer thickness is small as compared with the dimensions of the base-flow region is violated.

Physically, the high Mach number layers may be pictured as "bouncing" off of each other as they approach the neck. This phenomenon gives rise to a displacement of the zero streamline away from the axis and a decrease in the angle between the shear layer and the axis. This displacement increases with decreasing Reynolds number.

Although the simplified model of Chapman[24] predicts the correct order of magnitude for the base pressure, the dominant Reynolds number effect, which is not included in that model, makes numerical comparison meaningless.

V. Detailed Hot-Wire Measurements in the Near Wake of a Cylinder

Recovery Temperature Measurements

The hot-wire recovery temperature may be used to define the shear-layer thickness. The wire recovery temperature or the corresponding wire resistance as $i \to 0$ is a measure of the local stagnation temperature of the flow.[38]

Figure 13 shows the results of transverse surveys behind a cylinder at $x/D = 1.00$. The ratio $\bar{R} = (R - R_{lip})/(R_{lip} - R_{\mathbb{C}})$ at $i = 0$ has been used as a measure of the local stagnation temperature through the shear layer. R_{lip} is the measured resistance at the inner edge of the lip shock emanating from the separation point. These data are uncorrected for end loss to the supports and represent measurements obtained from three individual hot wires. $\bar{R}$ is essentially independent of both the end loss and the temperature-resistivity coefficient of the wire. This statement is proved by the coincidence of the solid and open inverted triangles. These points were obtained with two different wires operated at unit Reynolds numbers differing by a factor of 2.

The data indicate that the shear-layer thickness increases with decreasing Reynolds number. A "maximum slope thickness" may be defined by the intersection of the tangent to the $\bar{R}$ curve at its point of maximum slope with the values $\bar{R} = 0$ and $\bar{R} = 1$. For the five curves shown in the figure, the maximum slope thickness is proportional to $(Re_{\infty,D})^{-1/2}$. The region of inviscid flow between the edge of the shear layer and the lip shock rapidly disappears with decreasing Reynolds number. The position of the lip shock is nearly independent of Reynolds number, corroborating the surface-pressure data of Fig. 10 which show the separation point to be a weak function of Reynolds number.

A minimum value of $\bar{R}$ is associated with the zero-velocity point in the shear-layer profile. Consider the energy balance for a fine wire supported by two needles that are maintained at a temperature less than the local stagnation temperature of the flow. As the wire current approaches zero, the remaining heat-transfer mechanisms are convection from the stream to the wire, thermal conduction from the fluid to the wire, radiation from the wire to the cold walls of the wind tunnel, and solid body conduction from the wire to the supports. For these tests, radiation effects are unimportant so that a minimum in the wire resistance corresponds to a minimum in the convective heat transfer and, a fortiori, the point of zero velocity in the shear layer.

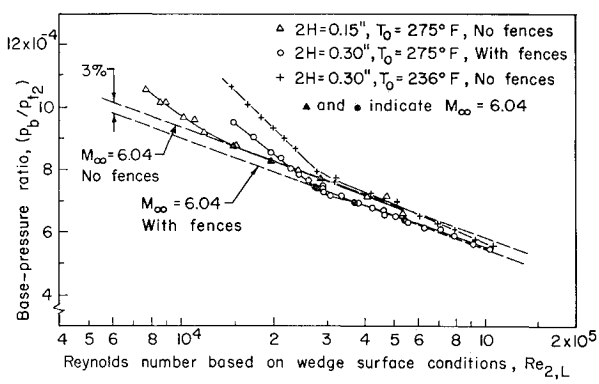

Fig. 11 Base pressure for a 15° half-angle wedge.

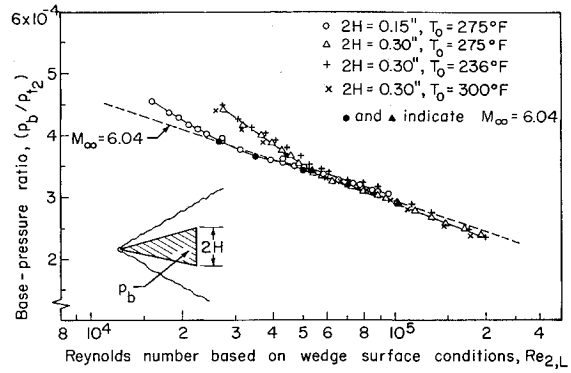

Fig. 12 Base pressure for a 22.5° half-angle wedge.

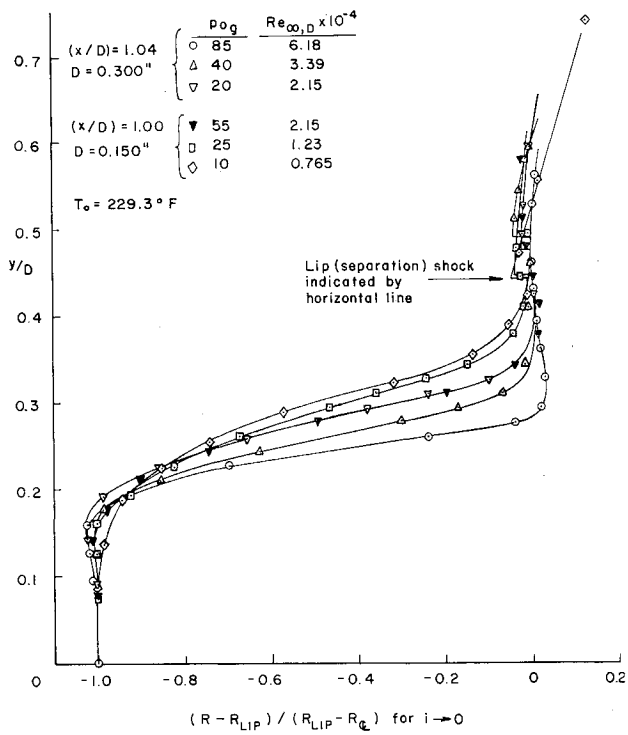

Fig. 13 Effect of Reynolds number on shear-layer thickness.

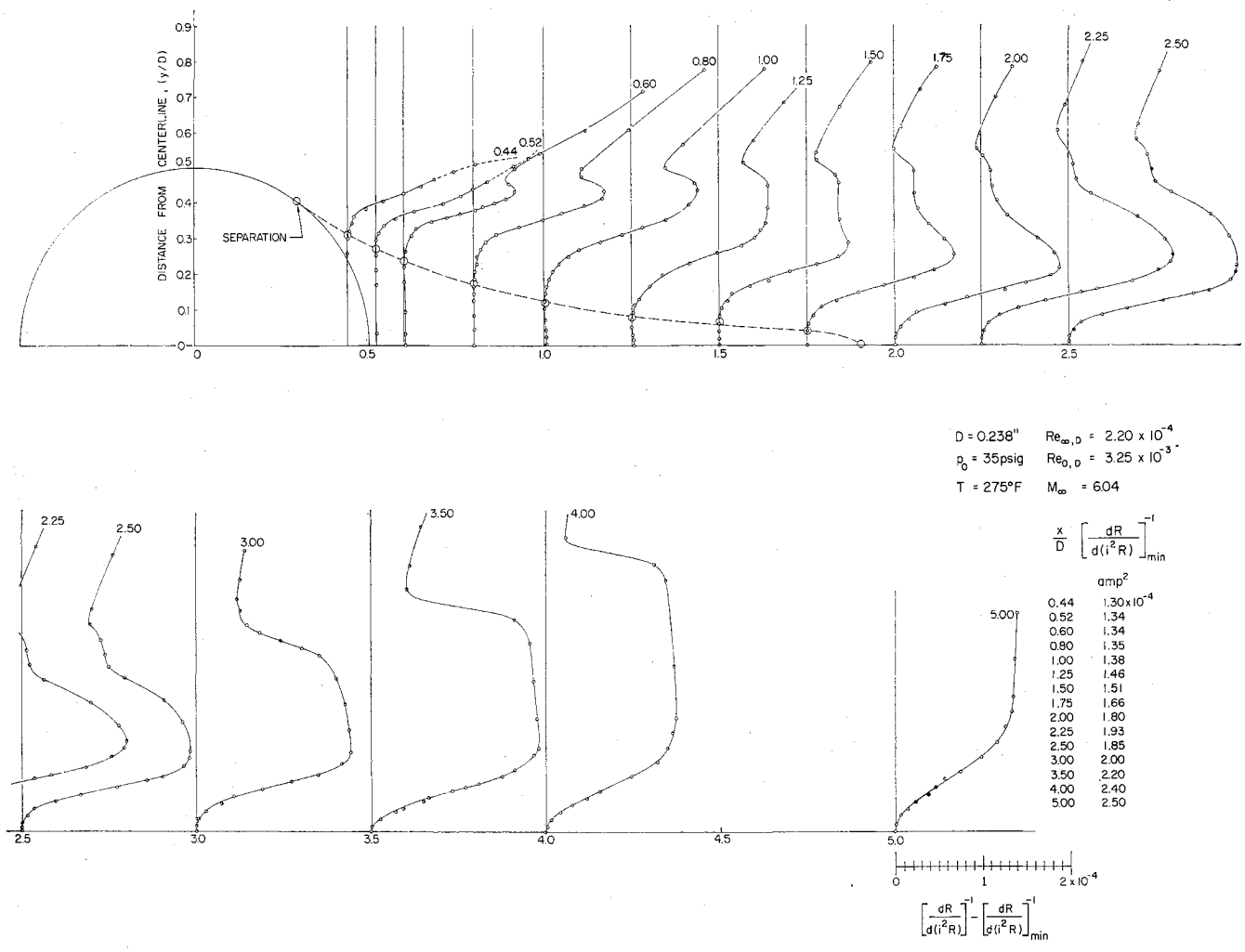

Fig. 14 Hot-wire map of the near wake of a circular cylinder.

Figure 13 indicates that the zero-velocity point at $x/D = 1.0$ is located at $y/D = 0.16$ and is independent of Reynolds number over the range investigated. The temperature level below the zero-velocity point rises rapidly to a constant value, which is maintained near the axis. This behavior is evidence for a small core of low-velocity reverse flow that eventually is brought to rest at the rear of the cylinder. This interpretation is subject to some question since the hot-wire supports may disturb the reverse flow passing over the hot wire. The magnitude of this disturbance is judged to be small because of the careful design of the hot-wire probe.

Heat-Loss Measurements

The data presented thus far have provided an insight into the changes in the near wake associated with changes in Reynolds number. Figure 14 presents a hot-wire map of the near wake of a cylinder at a Reynolds number $Re_{0,D} = 3.25 \times 10^3$. Profiles of the hot-wire heat loss $[dR/d(i^2R)]^{-1}$ are presented for stations $0.44 \leq x/D \leq 5$. Each trace is plotted to the scale shown at the bottom of station $x/D = 5$.

To aid in interpreting the data, the abscissa of each profile was placed so that the minimum value of $[dR/d(i^2R)]^{-1}$ was located at the (x/D) station where the traverse was obtained. Recovery resistance profiles were also obtained at each station. These curves showed distinct off-axis minimums similar to those shown in Fig. 13 for $x/D < 2$. The locations of the minimums are shown as large circles in the (x/D)-(y/D) plane and are connected by the line marked $u = 0$. This line is extended to that point on the trace of the body which marks the surface-pressure minimum for this Reynolds number, i.e., the approximate location of separation.

It is useful to consider the heat-loss difference $[dR/d(i^2R)]^{-1} - [dR/d(i^2R)]_{min}^{-1}$ as being a measure of the local mass flow. This statement is not precisely true, since the data are uncorrected for end losses and were obtained with several different wires, but it is qualitatively correct and provides a straightforward interpretation of the several features exhibited by the data.

Because of the curved bow shock wave, the inviscid flow outside the shear layer is highly rotational. The large inviscid gradients are evidenced by the slope of the heat-loss profiles for $(y/D) > 0.5$.¶ The location of the lip shock is evidenced by a sharp "valley" in the heat-loss data. The local minimum at the lip shock corresponds to the outer edge of this weak compression wave. Pitot-pressure traces and schlieren photographs have confirmed that this wave is not a sharp discontinuity but has a finite width that decreases with increasing Reynolds number. The path of the lip shock is seen to be a straight line with a virtual origin at the outer edge of the boundary layer at the separation point; the lip shock meets and is swallowed up by the emerging wake shock at $(x/D) = 3.00$.

The lip shock and the shear layer are merged near separation. At $(x/D) = 1.00$, an inviscid region begins to appear between the two. The inviscid region is distinct, and its

¶ The outer portions of the heat-loss profiles at $(x/D) = 0.44$ and 0.52 were disturbed by the presence of a goal-post wire and are shown as dotted lines. All of the other data were obtained without this disturbance.

extent is clearly evident in the heat-loss data $(x/D) = 1.00$ and 1.25.

A compression and turning of the flow is seen to begin at $(x/D) = 1.50$. The compression "hump" at the outer edge of the shear layer increases in magnitude and propagates outward as the neck region is approached. At $(x/D) = 2.00$, the two shear layers have merged, whereas the compression process at the outer edge of the viscous region is essentially complete at $(x/D) = 2.50$. The steepness of the compression front increases in the streamwise direction. Beyond $(x/D) = 3.00$, the compression maintains the characteristic form of a wake shock.

A detailed examination of the profiles in the base-flow region reveals several interesting features. From the requirement of mass conservation, the zero streamline and zero-velocity lines are required to form a wake stagnation point at the point of confluence of the two shear layers. From the trajectory of the $u = 0$ curve (which is not a streamline), the wake stagnation point is found to be located between $(x/D) = 1.75$ and $(x/D) = 2.00$; it is tentatively placed at $(x/D) = 1.90$. Kubota[45] has examined the flow in the vicinity of this point using the full Navier-Stokes equations. He finds that both the zero streamline and zero-velocity line must approach the axis vertically, and this fact has been utilized in drawing the $u = 0$ curve.**

The heat-loss profiles exhibit a small increase below the zero-velocity line. This behavior is attributed to the reverse flow in this region. The magnitude of this increase is very uncertain because end losses and thermal conduction comprise the bulk of the heat transfer in this region. Traverses at higher Reynolds numbers, for which the end losses of the hot wire were smaller, indicated that the reverse flow region is clearly marked by a small increase in the hot-wire heat loss. The location of the heat-loss minimum coincides with the point of minimum wire temperature and is identified with the point of zero velocity.

The heat-loss data reveal that a minimum in the wake thickness occurs at approximately $(x/D) = 2.7$; the wake stagnation point is located at $(x/D) = 1.9$. The action of significant viscous forces in the neck region is therefore indicated, at least for this low Reynolds number. Recent calculations by Lees and Reeves[47] have shown that the pressure rise at the neck requires several shear-layer thicknesses to approach its downstream value, and the length of the recompression increases with increasing M_e.

To summarize the results obtained from the hot-wire heat-loss measurements as supported by recovery temperature and surface-pressure studies, the following may be stated: 1) at low Reynolds numbers, the penetration of the shear layer into the base-flow region is extensive and increases with increasing M_e; 2) the neck compression region extends for several shear-layer thicknesses upstream and downstream of the wake stagnation point; 3) a distinct reverse flow exists in the interior of the base-flow region; and 4) the inviscid region outside the shear layer becomes less distinct as the Reynolds number decreases. Below $Re_{0,D} \approx 10^3$, an inviscid flow between the shear layer and the lip shock can no longer be identified, and the base-flow region contains large pressure gradients.

Appendix: A Goal-Post Technique for Mapping Streamlines

The 0.238-in.-diam cylinder had two 0.009-in.-diam needles projecting 0.0501 in. from the surface and placed 0.500 in. apart along a common surface generator. A platinum wire 0.001 in. in diameter was soft-soldered to the two needles, forming a crossbar between the two goal posts. By rotating the cylinder, the wire could be placed at successive positions

** More recently, Cheng[46] has arrived at a similar conclusion independently.

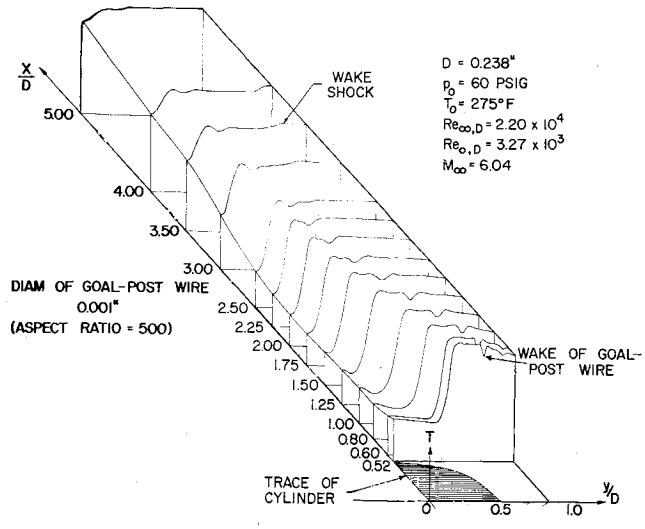

Fig. 15 The goal-post technique for mapping streamlines.

in the near-wake flow field. Just as the parent cylinder leaves a characteristic wake in the uniform flow of the wind tunnel, the satellite wire leaves a wake in the parent flow field. The wake of this goal-post wire will follow a streamline of the parent flow; if the small wake does not spread rapidly, the trace of the streamline will be distinct.

Figure 15 shows the temperature wake of the goal-post wire located outside the shear layer of the parent flow field. The three coordinates of this projection are (x/D), (y/D), and voltage of the hot wire used to survey the hybrid flow field. The hot wire was operated at a constant current of 1.000 ma so that the voltage was proportional to wire resistance, which, in turn, was linearly related to the recovery temperature of the wire. The maximum "bucket" in the parent wake temperature profile is about 30° C, corresponding to a 3% change in the hot-wire resistance.

The wake of the goal-post wire is very distinct in the first three diameters of the main base-flow region. Even fine details, such as wake shocks and an overshoot in total temperature at the outer edge of the satellite wake (since $Pr < 1$), may be recognized. This miniature wake eventually becomes absorbed by the main wake. The process begins for this particular goal-post position at about $(x/D) = 3$; the small wake is barely discernible at $(x/D) = 5$.

Within certain limitations, this technique offers the possibility of mapping flow streamlines with great facility. The first requirement is that the drag of the goal-post wire be small as compared with the momentum defect of the near wake. For a cylinder or other blunt body, a large portion of the initial drag appears in the inviscid flow so that the momentum defect produced by the bow shock of the satellite body is added to the momentum defect of the main base-flow region. In the present experiment, this produced a small but measurable translation of the main flow away from the side containing the disturbance. Second, the aspect ratio of the wire and the local Mach number of the flow approaching the goal-post wire must be large. If these conditions are not satisfied, the gross perturbations produced by the supports will significantly change the profile of the main wake. Finally, the spreading of the wake must be small so that a single streamline is identified. Otherwise, the existence of large gradients in the parent flow will make interpretation of the structure of the small wake very difficult.

References

[1] Roshko, A., "On the development of turbulent wakes from vortex streets," NACA TN 2913 (1950).

[2] Roshko, A., "On the drag and shedding frequency of two-dimensional bluff bodies," NACA TN 3169 (1959).

[3] Gorecki, J. P., "An investigation of temperature fluctuations on bluff bodies," Ph.D. Thesis, California Institute of Technology, Pasadena, Calif. (1960).

[4] Nash, J. F., "A review of research on two-dimensional base flow," National Physical Lab., Aeronautics Rept. 1006, A.R.C. 23649, F.M. 3171 (March 1962).

[5] Thomann, H., "Measurements of the recovery temperature in the wake of a cylinder and of a wedge at Mach numbers between 0.5 and 3," FFA (Sweden) Rept. 84 (1959).

[6] Gowen, F. E. and Perkins, E. W., "Drag of circular cylinders for a wide range of Reynolds numbers and Mach numbers," NACA TN 2960 (1953).

[7] Margevy, R. H. and Bishop, R. L., "Wakes in liquid-liquid systems," Phys. Fluids **4**, 800–805 (1961).

[8] McMahon, H., private communication to T. Kubota (September 19, 1960).

[9] Charters, A. C. and Thomas, R. N., "The aerodynamic performance of small spheres from subsonic to high supersonic velocities," J. Aerospace Sci. **12**, 468–476 (1945).

[10] Charters, A. C., private communication to L. Lees (1956).

[11] Pallone, A., Erdos, J., and Eckerman, J., "Hypersonic laminar wakes and transition studies," AIAA J. **2**, 855–863 (1964).

[12] Hayes, W. D. and Probstein, R. F., *Hypersonic Flow Theory* (Academic Press Inc, New York, 1959).

[13] Lees, L., "Hypersonic wakes and trails," AIAA J. **2**, 417–428 (1964).

[14] Slattery, R. C. and Clay, W. G., "Experimental measurement of turbulent transition, motion, statistics, and gross radial growth behind hypervelocity objects," Phys. Fluids **5**, 849–855 (1962).

[15] Demetriades, A. and Gold, H., "Transition to turbulence in the hypersonic wake of blunt-bluff bodies," ARS J. **32**, 1420–1421 (1962).

[16] Webb, W. H., Hromas, L., and Lees, L., "Hypersonic wake transition," AIAA J. **1**, 719–721 (1963).

[17] Gold, H., "Stability of laminar wakes," Ph.D. Thesis, California Institute of Technology, Pasadena, Calif. (1963).

[18] Gold, H., "Stability of axisymmetric laminar wakes," *AIAA Entry Technology Conference* (American Institute of Aeronautics and Astronautics, New York, October 1964), pp. 195–208.

[19] Chapman, D. R., "Base pressure at supersonic velocities," Ph.D. Thesis, California Institute of Technology, Pasadena, Calif. (1948).

[20] Crocco, L. and Lees, L., "A mixing theory for the interaction between dissipative flows and nearly isentropic streams," J. Aerospace Sci. **19**, 649–676 (1952).

[21] Glick, H. S., "Modified Crocco-Lees mixing theory for supersonic separated and reattaching flows," J. Aerospace Sci. **29**, 1238–1249 (1962).

[22] Chapman, D. R., "Laminar mixing of a compressible fluid," NACA Rept. 958 (1950).

[23] Chapman, D. R., "An analysis of base pressure at supersonic velocities and comparison with experiment," NACA Rept. 1051 (1951); supersedes NACA TN 2137 (1959).

[24] Chapman, D. R., Kuehn, D. M., and Larson, H. K., "Investigation of separated flows in supersonic and subsonic streams with emphasis on effect of transition," NACA Rept. 1356 (1958); supersedes NACA TM A 55L14 (1956) and NACA TN 3869 (1957).

[25] Korst, H. H., Page, R. H., and Childs, M. E., "Compressible two-dimensional jet mixing at constant pressure," Univ. of Illinois, Mechanical Engineering Dept. ME TN 392-1 (1954); also Korst, H. H., "Comments on the effect of boundary layer on sonic flow through an abrupt cross-sectional area change," J. Aerospace Sci. **21**, 568–569 (1954).

[26] Herzog, R. T., "Nitrogen injection into the base region of a hypersonic wake," Graduate Aeronautical Labs., California Institute of Technology Hypersonic Research Project, Memo. 71 (August 15, 1964).

[27] Kubota, T. and Dewey, C. F., Jr., "Momentum integral methods for the laminar free shear layer," AIAA J. **2**, 625–629 (1964).

[28] Denison, M. R. and Baum, E., "Compressible free shear layer with finite initial thickness," AIAA J. **1**, 342–349 (1963).

[29] Dewey, C. F., Jr., "Measurements in highly dissipative regions of hypersonic flows. Part II. The near wake of a blunt body at hypersonic speeds," Ph.D. Thesis, California Institute of Technology, Pasadena, Calif. (1963).

[30] Lees, L. and Reeves, B. L., "Supersonic separated and reattaching laminar flows: I. General theory and application to adiabatic boundary-layer shock-wave interactions," AIAA J. **2**, 1907–1920 (1964).

[31] McCarthy, J. F., Jr., "Hypersonic wakes," Graduate Aeronautical Labs., California Institute of Technology Hypersonic Research Project, Memo. 67 (July 2, 1962); also McCarthy, J. F., Jr. and Kubota, T., "A study of wakes behind a circular cylinder at $M = 5.7$," AIAA J. **2**, 629–636 (1964).

[32] Kingsland, L., Jr., "Experimental study of helium and argon diffusion in the wake of a circular cylinder at $M = 5.8$," Graduate Aeronautical Labs., California Institute of Technology Hypersonic Research Project, Memo. 60 (June 1, 1961).

[33] Tewfik, O. K. and Geidt, W. H., "Heat transfer, recovery factor, and pressure distribution around a cylinder normal to a supersonic rarefied air stream: Part I Experimental data," Univ. of California (Berkeley), TR HE-150-162 (January 30, 1959).

[34] Walter, L. W. and Lange, A. H., "Surface temperature and pressure distributions on a circular cylinder in supersonic cross-flow," Naval Ordance Lab. Rept. NAVORD 2854 (June 5, 1953).

[35] Gregorek, G. M. and Kordan, K. D., "An experimental observation of the Mach- and Reynolds-number independence of cylinders in hypersonic flow," AIAA J. **1**, 210–211 (1963).

[36] Holder, D. W. and Gadd, G. E., "The interaction between shock waves and boundary layers, and its relation to base pressure in supersonic flow," *Proceedings of the National Physical Laboratory International Symposium on Boundary Layer Effects in Aerodynamics* (Philosophical Library, London, 1957).

[37] Lees, L. and Hromas, L., "Turbulent diffusion in the wake of a blunt-nosed body at hypersonic speeds," J. Aerospace Sci. **29**, 976–993 (1962).

[38] Dewey, C. F., Jr., "Hot-wire measurements in low Reynolds number hypersonic flows," ARS J. **31**, 1709–1718 (1961).

[39] Kavanau, L. L., "Base pressure studies in rarefied supersonic flows," J. Aerospace Sci. **23**, 193–207, 230 (1956).

[40] Dewey, C. F., Jr., "Use of local similarity concepts in hypersonic viscous interaction problems," AIAA J. **1**, 20–32 (1963).

[41] Dewey, C. F., Jr., "A correlation of convective heat transfer and recovery temperature data for cylinders in compressible flow," Intern. J. Heat Mass Transfer **8**, 245–252 (1965).

[42] Beckwith, I. E. and Cohen, N. B., "Application of similar solutions to calculation of laminar heat transfer on bodies with yaw and large pressure gradient in high-speed flow," NASA TN D-625 (January 1961).

[43] Lees, L., "Laminar heat transfer over blunt-nosed bodies at hypersonic flight speeds," Jet Propulsion **26**, 259–269 (1956).

[44] Rom, J., "Theory for supersonic, two-dimensional laminar, base-type flows using the Crocco-Lees mixing concepts," J. Aerospace Sci. **29**, 963–965 (1962); also Rom, J. and Victor, M., "Correlation of the base-pressure behind a two-dimensional backward-facing step in a laminar supersonic flow," Technicon Aeronautical Engineering Rept. TAE–23 (December 1962).

[45] Kubota, T., private communication (June, 1962).

[46] Cheng, S. I., "Flow around an isolated stagnation point in the near wake," Avco/RAD TM-63-23 (Revision 1) (July 31, 1963).

[47] Lees, L. and Reeves, B. L., private communication (July 1963)